EPJ Web of Conferences **364**, 15006 (2026) https://doi.org/10.1051/epjconf/202636415006
Quark Matter 2025

Baryon-strangeness correlations in Au+Au collisions at RHIC-STAR

Hanwen Feng[1,*] for the STAR Collaboration

[1]Key Laboratory of Quark & Lepton Physics (MOE) and Institute of Particle Physics, Central China Normal University, Wuhan 430079, China

Abstract. Fluctuations and correlations of conserved charges are powerful probes of QCD thermodynamics and the phase structure of strongly interacting matter. Among them, the baryon-strangeness correlation, C_{BS}, has been proposed as a particularly sensitive indicator of changes in the underlying degrees of freedom in relativistic heavy-ion collisions. In this work, we present detailed correction procedures for C_{BS} from data collected by the STAR experiment at RHIC. This approach enables precise and reliable C_{BS} measurements to explore the QCD phase diagram.

1 Introduction

Mapping the QCD phase diagram is a primary goal of ultra-relativistic heavy-ion collisions [1–4]. While the chemical freeze-out curve is now well constrained [5, 6], first order phase transition (if exists) and the location of critical end point remain uncertain. Fluctuations and correlations of conserved charges offer sensitivity to the underlying degrees of freedom. In particular, it's suggested that baryon-strangeness correlations C_{BS} can distinguish the deconfined medium from a hadronic medium [7, 8]. This work outlines the STAR analysis framework for precise C_{BS} measurements. Here we discuss proxy charge construction and the purity, centrality bin width, and efficiency corrections.

2 Experimental Observable

Baryon-strangeness correlations, C_{BS}, is defined in terms of event-by-event fluctuations of the net baryon number B and net strangeness S:

$$C_{BS} = -3\frac{\langle BS\rangle_c}{\langle S^2\rangle_c} = -3\frac{\langle BS\rangle - \langle B\rangle\langle S\rangle}{\langle S^2\rangle - \langle S\rangle^2} \tag{1}$$

In an weakly-interacting quark-gluon plasma, strangeness is carried exclusively by strange quarks, leading to $C_{BS} \approx 1$ independent of the baryon chemical potential μ_B. While in the hadronic environment, C_{BS} is sensitive to the relative abundance of strange baryons and strange mesons, producing a μ_B dependence that rises with increasing strange baryon fraction.

*e-mail: hwfeng@mails.ccnu.edu.cn

As direct measurement of B and S in heavy-ion collisions is experimentally infeasible, we construct proxy charges from experimentally accessible hadrons:

$$B = \delta p + \delta\Lambda(+\delta\Xi^-) \qquad S = \delta K^+ - \delta\Lambda(-2\delta\Xi^-) \tag{2}$$

The validity of the proxy charge construction has been discussed in [9, 10], which confirms that the chosen particle sets are suitable for experimental determination of C_{BS}.

3 Correction Procedures

3.1 Purity Correction

Reconstruction of $\Lambda(\overline{\Lambda})$ and $\Xi^-(\overline{\Xi}^+)$ inevitably produces combinatorial background. Following Ref. [11], we subtract it using n background estimators R_i. Let N_B be the true background, N_{R_i} $(i = 1, \ldots, n)$ the i-th estimator, N_{SC} the signal candidates, and N_S the true signal. The correction formulas up to second-order are expressed as:

$$\begin{aligned} \langle N_S \rangle &= \langle N_{SC} \rangle - \langle N_{R_i} \rangle \\ \left\langle N_S^2 \right\rangle &= \left\langle N_{SC}^2 \right\rangle - \left\langle N_{R_i}^2 \right\rangle + 2\langle N_{SC} N_{R_i} \rangle - 2\langle N_{SC} N_{R_i} \rangle + 2\left\langle N_{R_i} N_{R_j} \right\rangle \end{aligned} \tag{3}$$

Multiple estimators are constructed using the side-bands, which refers to invariant mass regions outside the signal region. Each sideband is iteratively adjusted to minimize the difference between the left and right hand sides of Eq. 4:

$$\int_{Signal} N_{\text{Rotation}}(M_{Inv})\, \mathrm{d}M_{Inv} = \int_{Band} N_{\text{Reconstruction}}(M_{Inv})\, \mathrm{d}M_{Inv}. \tag{4}$$

Fig. 1 demonstrates that raw second-order Λ cumulants exhibit dependence on purity, which vanishes after correction, confirming effective removal of combinatorial background.

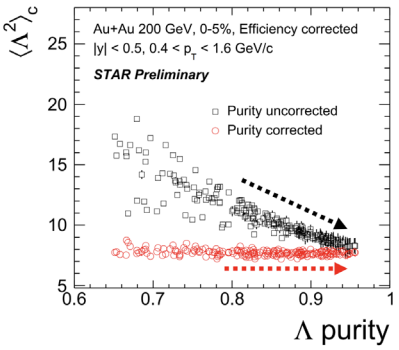

Figure 1. Second order cumulant of Λ under different purity. Results with purity correction are marked by red circles and the one without is represented by black squares.

3.2 Centrality Bin Width Correction

To suppress the Centrality Bin Width Effect (CBWE) arising from volume (participant) fluctuations inside a finite centrality bin, raw cumulants are first evaluated in the narrowest available multiplicity bins, then combined with event-count weights [12]:

$$\langle N_1^r N_2^s \ldots N_k^t \rangle_c = \sum_{i=1}^{n} w_i \langle N_1^r N_2^s \ldots N_k^t \rangle_{c,i}, \qquad w_i = N_{\text{evt}}^i / \sum_{j=1}^{n} N_{\text{evt}}^j. \tag{5}$$

We find in Fig. 2 that results in 9 centrality bins without CBWC clearly deviates from the one obtained directly from 32 fine multiplicity bins. In contrast, applying CBWC to 9 coarse centrality bins reproduces the fine-bin reference, indicating that CBWC effectively suppresses the centrality bin width bias.

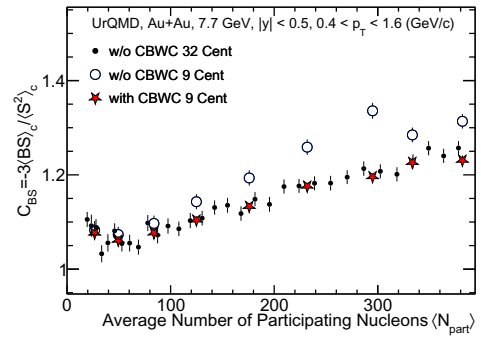

Figure 2. Demonstration of the Centrality Bin Width Correction (CBWC) using UrQMD Au+Au events at $\sqrt{s_{NN}}$ = 7.7 GeV. Cumulants from 9 wide centrality bins with CBWC reproduces the fine-bin result within statistical uncertainties.

3.3 Efficiency Correction

Due to limited detector acceptance and efficiency, the measured cumulants should be corrected by the method described in [13, 14]. Tracking efficiencies for p and $K^{\pm}$ (TPC) and topological reconstruction efficiencies for Λ and Ξ^{-} are obtained via MC embedding to capture acceptance and detector response. TOF matching efficiencies are derived with data-driven methods. We use clean TPC-selected samples to measure the probability that reconstructed TPC tracks have a matched TOF hit from data, independent of simulation.

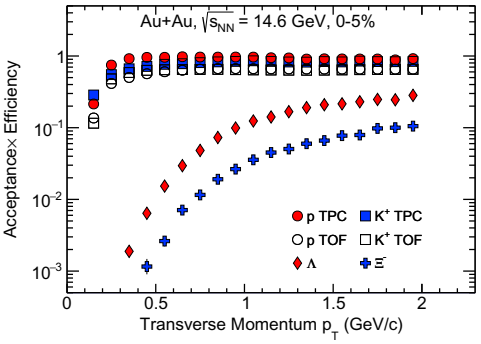

Figure 3. Estimated tracking efficiency of $p, K^{\pm}$ in TPC and reconstruction efficiency of Λ, Ξ^{-} in 0-5% Au+Au collisions at 14.6 GeV.

4 Summary and Outlook

We have presented correction procedures to improve the measurements of baryon-strangeness correlation in heavy-ion collisions, including purity corrections, centrality bin width corrections, and efficiency corrections. The application of these methods can lead to more reliable results and help us understand the QCD phase diagram and properties of the quark-gluon plasma. Furthermore, contributions from feed-down processes should be taken into account in future analyses.

Acknowledgments

We thank the RHIC Operations Group and RCF at BNL. This work was supported by National Key Research and Development Program of China (No.2022YFA1604900), National Natural Science Foundation of China (NO. 12525509 and 12447102).

References

[1] A. Bzdak, S. Esumi, V. Koch, J. Liao, M. Stephanov, N. Xu, Mapping the Phases of Quantum Chromodynamics with Beam Energy Scan, Phys. Rept. **853**, 1 (2020). 10.1016/j.physrep.2020.01.005

[2] X. Luo, Q. Wang, N. Xu, P. Zhuang, eds., Properties of QCD Matter at High Baryon Density (Springer, 2022), ISBN 978-981-19-4440-6, 978-981-19-4443-7, 978-981-19-4441-3

[3] J. Chen et al., Properties of the QCD matter: review of selected results from the relativistic heavy ion collider beam energy scan (RHIC BES) program, Nucl. Sci. Tech. **35**, 214 (2024). 10.1007/s41365-024-01591-2

[4] X. Luo, N. Xu, Search for the QCD Critical Point with Fluctuations of Conserved Quantities in Relativistic Heavy-Ion Collisions at RHIC : An Overview, Nucl. Sci. Tech. **28**, 112 (2017). 10.1007/s41365-017-0257-0

[5] J. Cleymans, K. Redlich, Chemical and thermal freezeout parameters from 1-A/GeV to 200-A/GeV, Phys. Rev. C **60**, 054908 (1999). 10.1103/PhysRevC.60.054908

[6] A. Andronic, P. Braun-Munzinger, K. Redlich, J. Stachel, Decoding the phase structure of QCD via particle production at high energy, Nature **561**, 321 (2018). 10.1038/s41586-018-0491-6

[7] M. Asakawa, U.W. Heinz, B. Muller, Fluctuation probes of quark deconfinement, Phys. Rev. Lett. **85**, 2072 (2000). 10.1103/PhysRevLett.85.2072

[8] V. Koch, A. Majumder, J. Randrup, Baryon-strangeness correlations: A Diagnostic of strongly interacting matter, Phys. Rev. Lett. **95**, 182301 (2005). 10.1103/PhysRevLett.95.182301

[9] R. Bellwied, S. Borsanyi, Z. Fodor, J.N. Guenther, J. Noronha-Hostler, P. Parotto, A. Pasztor, C. Ratti, J.M. Stafford, Off-diagonal correlators of conserved charges from lattice QCD and how to relate them to experiment, Phys. Rev. D **101**, 034506 (2020). 10.1103/PhysRevD.101.034506

[10] J. Jahan, C. Ratti, M. Stefaniak, K. Werner, New proxies for second-order cumulants of conserved charges in heavy-ion collisions within the EPOS4 framework, Phys. Rev. C **110**, 035201 (2024). 10.1103/PhysRevC.110.035201

[11] T. Nonaka, Purity correction for cumulants of hyperon number distribution, Nucl. Instrum. Meth. A **1039**, 167171 (2022). 10.1016/j.nima.2022.167171

[12] X. Luo, J. Xu, B. Mohanty, N. Xu, Volume fluctuation and auto-correlation effects in the moment analysis of net-proton multiplicity distributions in heavy-ion collisions, J. Phys. G **40**, 105104 (2013). 10.1088/0954-3899/40/10/105104

[13] X. Luo, T. Nonaka, Efficiency correction for cumulants of multiplicity distributions based on track-by-track efficiency, Phys. Rev. C **99**, 044917 (2019). 10.1103/PhysRevC.99.044917

[14] A. Bzdak, R. Holzmann, V. Koch, Multiplicity-dependent and nonbinomial efficiency corrections for particle number cumulants, Phys. Rev. C **94**, 064907 (2016). 10.1103/PhysRevC.94.064907